

Mixed Elements, Stress Fields and Failure Parameters in Laminated Anisotropic Plates

E. Carrera^a, P. Nali^b, A. Buettner^c

^a Professor, “Politecnico di Torino”

Dipartimento di Ingegneria Aerospaziale

e.mail: erasmo.carrera@polito.it - website: www.polito.it/mul2

^b PhD Student, “Politecnico di Torino”

Dipartimento di Ingegneria Aerospaziale

e.mail: pietro.nali@polito.it - website: www.polito.it/mul2

^c MSc Student, “University of Stuttgart” - Institut für Statik und Dynamik der Luft- und Raumfahrttechnik

e.mail: axelbuettner@gmx.de

Abstract

This paper is devoted to evaluating various benchmark problems that make the advantages of the multilayered composite plate hierarchical theories based on the Carrera Unified Formulation evident. Attention is in particular focused on the implementation and use of layer-wise FEs. Both classical and mixed variational statements are considered for comparison purposes. The stress field is evaluated and compared to three-dimensional elasticity solutions. The maximum stress criterion is applied to evaluate the maximum loading related to the first ply failure. Orthotropic as well as anisotropic plates have been analyzed.

1. Introduction

It is an established fact that further advances in the use of laminates composites are subordinate to a better understanding of their failure mechanisms. On the other hand, the analysis and simulation of the failure of composite laminated structures are quite cumbersome tasks. The failure mechanisms are very different from those of traditional metallic structures. The combination of various interfaces (fibers, matrix, layers) at a macro scale level requires a local dedicated analysis to establish the initiation of failure mechanisms of a fiber, crack in the matrix or delamination between two different layers. The following list of points could be considered.

1. Calculation of the failure initiation, which is only the very first difficulty.
2. Evolution of failure, also called “progressive failure” is the next fundamental step. Failure evolution can follow various paths: a crack in the matrix can lead to rupture of the fiber or to a delamination; a delamination can lead to a crack in the matrix etc.

3. The third step would be the analysis of the interaction of failures/cracks: how many cracks are there? How do they propagate? How do they interact with each other?
4. The fourth step would be to describe how the various types of damage (initiation, evolution, interaction) grow if loading is varied in time; that is, design to fatigue has to be considered.
5. The fifth point is the dependence of the previous factors on environmental effects such as temperature, humidity absorption, electric charge, etc.

The previous five points, which have been quite well established and handled for metallic structures, are, unfortunately, far from being solved for composites made structures. Extensive use of experiments is made in most advanced composite constructions. Quite expensive test campaign have been conducted for composite made parts of aircrafts such as A350 or B787. Due to intrinsic tailoring, anisotropy and lay-out, the number of necessary experiments has increased remarkably with respect to traditional metallic structures. Uncertainties could play a predominant role in both experiments and analysis. Many additional sources of uncertainties in fact arise, such as angle of fiber orien-

tation, ply thickness, and mechanical/thermal/electric properties of the lamina (fiber and matrix).

Due to the above mentioned complicating effects, various Regulation Authorities have introduced severe safety rules and regulations in the design and use of composite materials. It appears mandatory that future years should be devoted to a better understanding of the above mentioned topics. Nevertheless, thousand of contributions are already available.

Although the evaluation of stress fields in laminates is not the final point for their improved design and use, the accurate calculation of stresses, strains and displacements plays a fundamental role, at least in predicting failure initiation. The most fundamental contribution to this topic remains the book by Leckhniskii [1]. Many fundamental and singular stress problems are analyzed and solved in this book. More recent studies have been conducted by numerous scientists; among these, the works by Pagano should be mentioned [2],[3].

Although many refined models have been developed (see works [4]-[7]), most of the available FEM general purpose codes still evaluate the stress field by employing classical theories, such as the FSDT (First, order Shear Deformation Theory), which is based on Reissner-Mindlin type assumptions, see [8]; the FSDT neglects transverse normal strain and violates interlaminar continuity of transverse shear stress components. However, the plate theories currently implemented in commercial codes are all formulated following the Equivalent Single Layer (ESL) approach, which can be appropriate to analyze conventional one-layered panels, but fails when a multilayered composite structure is addressed (especially if accurate interlaminar stress or failure results are needed). Many theories have been formulated employing the so-called Layer-Wise (LW) approach, which consists of a more advanced kinematic description (each layer is considered independently of the others) and also leads to accurate results for multilayered composite plates [9]. In the framework of the accurate evaluation of stress fields, the first author has shown that the Reissner Mixed Variational Theorem (RMVT) [10] consists of a natural extension of the Principle of Virtual Displacements (PVD) to multilayered structure analysis (beams, plates, shells) [11]. A large variety of mixed theories and computational models have been developed and applied, see [12]. The present work has the aim of showing the capability of the RMVT to develop plate FEs which lead to a three-dimensional description of the stress field in laminated structures. Both ESL and LW variable description have been adopted. The order of the expansion N is considered, in all cases, as a free parameter of the investigation. All the above modellings are implemented with reference to the Carrera Unified Formulation (CUF) [13],[14]. This formulation permits one to obtain the FE ma-

trices in terms of fundamental nuclei, whose form is independent of the choice of the thickness functions $F_T(z)$, order, element number of nodes and the variable description (ESL, LW). With respect to previous work, the present contribution introduces mixed elements with the use of Lagrange Polynomials and applies them to the evaluation of failure parameters.

Various in-house software programs based on CUF have been developed and applied to different problems. These codes have recently been included in a research platform called MUL2. This platform has partially been sponsored by ESA-ESTEC through the funding of the PhD research work of the second author. The classical Lamination Theory (CLT), First order Shear Deformation Theory (FSDT), High Order Shear Deformation Theories (HOSDTs), Zig-Zag theories [15], LW Theories as well as mixed models based on the RMVT are all included in MUL2, which can be considered an academic platform to compare a considerable set of different plate theories. The paper has been organized as follows. The Reissner Mixed Variational Theorem is introduced in Sec. 2. Sec. 3 describes the considered plate theories based on CUF. Constitutive equations and geometrical relations for RMVT modelling are listed in Sec. 4. FE matrices are obtained in Sec. 5. Failure criteria are introduced in Sec. 6. The numerical results are illustrated in Sec. 7.

2. Variational statements

Equilibrium in a laminated structure can be obtained by the application of the PVD. For a multilayered plate it takes the following form:

$$\sum_{k=1}^{N_L} \int_{\Omega_k} \int_{h_k} (\delta \varepsilon_p^{kT} \sigma_p^k + \delta \varepsilon_n^{kT} \sigma_n^k) d\Omega_k dz = \delta L_e, \quad (1)$$

where the cartesian x , y , z reference system is considered, the z coordinate is along the plate-thickness direction, δ is the variational symbol, h_k is the thickness of the k -th layer, N_L is the number of layers and Ω_k is the plate surface. The left part represents the virtual variation of the internal work L_i while L_e is the work made by external loads. Internal work has been conveniently split into in-plane and out-of plane contributions. Therefore stresses and strains are separated to in-plane and transverse components denoted by the subscript p and n respectively:

$$\begin{aligned} \sigma_p &= [\sigma_{xx}, \sigma_{yy}, \sigma_{xy}]^T & \sigma_n &= [\sigma_{xz}, \sigma_{yz}, \sigma_{zz}]^T \\ \varepsilon_p &= [\varepsilon_{xx}, \varepsilon_{yy}, \varepsilon_{xy}]^T & \varepsilon_n &= [\varepsilon_{xz}, \varepsilon_{yz}, \varepsilon_{zz}]^T \end{aligned} \quad (2)$$

The virtual variation of the external work can be expressed as:

$$\delta L_e = \int_{\Omega} (\delta u^T \bar{t}) d\Omega, \quad (3)$$

where \bar{t} is the mechanical loading vector of applied pressure and u is the vector of displacements. The

PVD application permits to assume only displacement variables. Reissner [10] proposed to additionally enforce compatibility of transverse normal strain variables by the following RMVT:

$$\int_V [\delta \varepsilon_{pG}^T \sigma_{pC} + \delta \varepsilon_{nG}^T \sigma_{nM} + \delta \sigma_{nM}^T (\varepsilon_{nG} - \varepsilon_{nC})] dV = \delta L_e. \quad (4)$$

The index M now emphasizes that the normal stresses are assumed in the model. Strains which are calculated with geometrical relations are marked with the index G and the variables expressed by constitutive equations are denoted by the subscript C . To be noted that the normal strains ε_{nC} must be obtained from the constitutive equations and therefore the normally used Hooke's law must be transformed. With respect to PVD, the RMVT permits one to assume both displacement and transverse stress variables. These last are conveniently assumed continuous at each layer-interface by adopting a LW description.

3. Layer-wise description based on CUF

In a LW model the thickness expansion is performed for each layer separately so that independent variables are assumed for each layer k . The interlaminar continuity must be imposed for each layer interface but the gradients at the layer interfaces can differ. According to the RMVT, displacement and stress variables are introduced in the following form:

$$u^k = F_t u_t^k + F_b u_b^k + F_r u_r^k = F_\tau u_\tau^k \quad (5)$$

$$\sigma_{nM}^k = F_t \sigma_{nt}^k + F_r \sigma_{nr}^k + F_b \sigma_{nb}^k = F_\tau \sigma_{n\tau}^k, \quad (6)$$

where $\tau = t, b, r$;

$$r = 2, 3, \dots, N \quad \text{and} \quad k = 1, 2, \dots, N_L.$$

F_τ are the base functions for the expansion in thickness-direction z . The interlaminar continuity of the displacements and transverse stresses is imposed straightforwardly:

$$u_t^k = u_b^{(k+1)}, \quad \text{with} \quad k = 1, \dots, N_L - 1; \quad (7)$$

$$\sigma_{nt}^k = \sigma_{nb}^{k+1} \quad \text{for} \quad k = 1, \dots, N_L - 1, \quad (8)$$

where top and bottom of the layer are denoted with subscripts t and b , respectively. In next section a possible polynomial choice for the base functions F_τ is illustrated.

3.1. Combination of Legendre polynomials

For the base functions F_τ a combination of Lagrange polynomials is used, wherein ζ_k is the dimensionless thickness coordinate of the layer k , defined in the domain $-1 \leq \zeta_k \leq 1$. The Lagrange polynomials up to

4-th order are given in Tab. 1. The following properties are respected:

$$\begin{aligned} \zeta_k = 1 & : & F_t = 1; & F_r = 0; & F_b = 0; \\ \zeta_k = -1 & : & F_t = 0; & F_r = 0; & F_b = 1; \\ \zeta_k = z_i & : & F_t = 0; & F_i = 1; & F_{r \neq i} = 0; & F_b = 0. \end{aligned}$$

Unless otherwise noted, the parameters z_i for higher order Lagrange polynomials divide the domain $[-1, 1]$ in equal distances, i.e. for the 4-th order case:

$$\zeta_k(z_1) = -0.5; \quad \zeta_k(z_2) = 0.0; \quad \zeta_k(z_3) = 0.5.$$

The two Lagrange polynomials F_t and F_b refer to the top and bottom surface of each layer. Lagrange polynomials are characterized by only physical displacement as problem variables. Such an advantage could be particularly significant in nonlinear analysis since the related FEs lead to the zero-strain condition in case of rigid body motion. In this work, linear up to fourth order expansion are considered.

4. Constitutive equations and geometric relations for RMVT

For the sake of brevity, the governing equations are addressed assuming only the RMVT. For PVD, the procedure is done in perfect accordance with RMVT, details can be found in many articles, i.e. [11],[13]. The conventional Hooke's law for general material behavior states:

$$\begin{aligned} \sigma_p &= \tilde{C}_{pp} \varepsilon_p + \tilde{C}_{pn} \varepsilon_n \\ \sigma_n &= \tilde{C}_{np} \varepsilon_p + \tilde{C}_{nn} \varepsilon_n \end{aligned}, \quad (9)$$

where stresses and strains are already split to in-plane and transverse components denoted with the subscript p and n respectively. For the mixed model, transverse stresses are assumed and can not anymore be expressed in terms of the strains ε_p and ε_n . Hooke's law in Eqn.(9) has to be modified. The mixed formulation of the constitutive equations expresses σ_p and ε_n in terms of σ_{nM} and ε_p . They can be therefore written as:

$$\begin{aligned} \sigma_{pC}^k &= C_{pp}^k \varepsilon_{pG}^k + C_{pn}^k \sigma_{nM}^k \\ \varepsilon_{nC}^k &= C_{np}^k \varepsilon_{pG}^k + C_{nn}^k \sigma_{nM}^k \end{aligned}. \quad (10)$$

The elasticity arrays of the mixed equations are the followings:

$$C_{pp} = \tilde{C}_{pp} - \tilde{C}_{pn} \tilde{C}_{nn}^{-1} \tilde{C}_{np}; \quad C_{pn} = \tilde{C}_{pn} \tilde{C}_{nn}^{-1}; \quad (11)$$

$$C_{np} = -\tilde{C}_{nn}^{-1} \tilde{C}_{np}; \quad C_{nn} = \tilde{C}_{nn}^{-1}. \quad (12)$$

The geometric relations in linearized form are employed to express the strains ε_{pG} and ε_{nG} in terms of the displacements components in the vector $u = [u_x, u_y, u_z]^T$:

$$\varepsilon_{pG} = D_p u; \quad \varepsilon_{nG} = D_n u. \quad (13)$$

The arrays D_p and D_n contain the differential operators. Their explicit form is:

$$D_p = \begin{bmatrix} \partial_x & 0 & 0 \\ 0 & \partial_y & 0 \\ \partial_y & \partial_x & 0 \end{bmatrix}; \quad D_n = \begin{bmatrix} \partial_z & 0 & \partial_x \\ 0 & \partial_z & \partial_y \\ 0 & 0 & \partial_z \end{bmatrix}.$$

The differential operator array D_n can be split in in-plane and out-of-plane contributions:

$$D_n = D_{n\Omega} + D_{nz}, \quad (14)$$

with:

$$D_{n\Omega} = \begin{bmatrix} 0 & 0 & \partial_x \\ 0 & 0 & \partial_y \\ 0 & 0 & 0 \end{bmatrix}; \quad D_{nz} = \begin{bmatrix} \partial_z & 0 & 0 \\ 0 & \partial_z & 0 \\ 0 & 0 & \partial_z \end{bmatrix}.$$

5. Derivation of Finite Element Matrices

An exhaustive description of the derivation of FE matrices can be read in [14],[16]. For sake of completeness the fundamental nuclei for RMVT are obtained in the following.

5.1. FE discretization

If the FEM is employed, the vectors of the k-layer primary unknowns u_τ^k and σ_n^k can be expressed in terms of their nodal values $q_{\tau i}^k$ and $g_{\tau i}^k$. That is the problem is discretized via the shape functions N_i :

$$u_\tau^k(x, y) = N_i(x, y) q_{\tau i}^k, \quad i = 1, 2, \dots, N_n; \quad (15)$$

$$\sigma_{n\tau}^k(x, y) = N_i(x, y) g_{\tau i}^k, \quad i = 1, 2, \dots, N_n. \quad (16)$$

N_n denotes the number of nodes concerning the considered FE, $q_{\tau i}^k$ and $g_{\tau i}^k$ are the vectors of the nodal unknowns:

$$q_{\tau i}^k = [q_{u_x\tau i}^k, q_{u_y\tau i}^k, q_{u_z\tau i}^k]^T, \quad (17)$$

$$g_{\tau i}^k = [g_{xz\tau i}^k, g_{yz\tau i}^k, g_{zz\tau i}^k]^T. \quad (18)$$

Substituting Eqn. (15) in Eqn. (5), the final three-dimensional expression of the displacements field is obtained:

$$u^k(x, y, z) = F_\tau(z) N_i(x, y) q_{\tau i}^k. \quad (19)$$

The same proceeding can be done for the transverse stresses: substituting Eqn. (16) in Eqn. (6) leads to:

$$\sigma_{nM}^k(x, y, z) = F_\tau(z) N_i(x, y) g_{\tau i}^k. \quad (20)$$

5.2. FE fundamental nuclei

The RMVT application in Eqn. (4), restricted to the layer k takes the following form for a multilayered plate:

$$\sum_{k=1}^{N_L} \int_{\Omega_k} \int_{h_k} [\delta \varepsilon_{pG}^{kT} \sigma_{pC}^k + \delta \varepsilon_{nG}^{kT} \sigma_{nM}^k + \delta \sigma_{nM}^{kT} (\varepsilon_{nG}^k - \varepsilon_{nC}^k)] d\Omega_k dz = \delta L_e. \quad (21)$$

Introducing the Hooke's law for the mixed case of Eqn. (10), one gets:

$$\int_{\Omega_k} \int_{h_k} [\delta \varepsilon_{pG}^{kT} C_{pp}^k \varepsilon_{pG}^k + \delta \varepsilon_{pG}^{kT} C_{pn}^k \sigma_{nM}^k + \delta \varepsilon_{nG}^{kT} \sigma_{nM}^k + \delta \sigma_{nM}^{kT} \varepsilon_{nG}^k - \delta \sigma_{nM}^{kT} C_{np}^k \varepsilon_{pG}^k - \delta \sigma_{nM}^{kT} C_{nn}^k \sigma_{nM}^k] d\Omega_k dz = \delta L_e. \quad (22)$$

Considering the thickness expansion in Eqn. (5), the geometrical relations collected in the differential operator of Eqn. (13) and the FE discretization in Eqn. (15),(16), the strains ε_p and ε_n can be written as in the following:

$$\varepsilon_{pG}^k = F_\tau D_p(N_i I) q_{\tau i}^k \quad (23)$$

$$\varepsilon_{nG}^k = F_\tau D_{n\Omega}(N_i I) q_{\tau i}^k + F_{\tau,z} N_i q_{\tau i}^k \quad (24)$$

where $I = \begin{bmatrix} 1 & 0 & 0 \\ 0 & 1 & 0 \\ 0 & 0 & 1 \end{bmatrix}$ and $F_{\tau,z} = \frac{\partial F_\tau}{\partial z}$. Upon

substitution of Eqns. (23), (24) and (20) in Eqn. (22), the internal virtual work for the k -th layer takes the following form:

$$\begin{aligned} \delta L_i^k = & \triangleleft \{ \delta q_{\tau i}^{kT} [D_p^T(N_i I) Z_{pp}^{k\tau s} D_p(N_j I)] q_{s j}^k \} \triangleright_\Omega + \\ & + \triangleleft \{ \delta q_{\tau i}^{kT} [D_p^T(N_i I) Z_{pn}^{k\tau s} N_j] g_{s j}^k \} \triangleright_\Omega + \\ & + \triangleleft \{ \delta q_{\tau i}^{kT} [D_{n\Omega}^T(N_i I) E_{\tau s} N_j + E_{\tau,z} N_i N_j I] g_{s j}^k \} \triangleright_\Omega + \\ & + \triangleleft \{ \delta g_{\tau i}^{kT} [N_i E_{\tau s} D_{n\Omega}(N_j I) + E_{\tau s,z} N_i N_j I] q_{s j}^k \} \triangleright_\Omega + \\ & - \triangleleft \{ \delta g_{\tau i}^{kT} [N_i Z_{np}^{k\tau s} D_p(N_j I)] q_{s j}^k \} \triangleright_\Omega + \\ & - \triangleleft \{ \delta g_{\tau i}^{kT} [N_i Z_{nn}^{k\tau s} N_j] g_{s j}^k \} \triangleright_\Omega. \end{aligned} \quad (25)$$

Subscripts τ and i are related to virtual variations, while subscript s and j concern the true quantities. The symbol $\triangleleft \dots \triangleright_\Omega$ denotes the integral on Ω . As usual in two-dimensional modelling, the integration through the thickness-direction can be made a priori. The below layer-integrals are introduced in Eqn. (25):

$$\begin{aligned} & (E_{\tau s}, E_{\tau s,z}, E_{\tau,z} s, E_{\tau,z} s,z) = \\ & = \int_{h_k} (F_\tau F_s, F_\tau F_{s,z}, F_{\tau,z} F_s, F_{\tau,z} F_{s,z}) dz. \end{aligned} \quad (26)$$

If the following laminate stiffness definitions are considered:

$$(Z_{pp}^{k\tau s}, Z_{pn}^{k\tau s}, Z_{np}^{k\tau s}, Z_{nn}^{k\tau s}) = (C_{pp}^k, C_{pn}^k, C_{np}^k, C_{nn}^k) E_{\tau s},$$

Eqn. (25) can be written in the compact form:

$$\delta L_i^k = \delta q_{\tau i}^{kT} [K_{uu}^{k\tau s i j} q_{s j}^k + K_{u\sigma}^{k\tau s i j} g_{s j}^k] + \delta g_{\tau i}^{kT} [K_{\sigma u}^{k\tau s i j} q_{s j}^k + K_{\sigma\sigma}^{k\tau s i j} g_{s j}^k]. \quad (27)$$

where:

$$\begin{aligned} K_{uu}^{k\tau s i j} &= \triangleleft [D_p^T(N_i I) Z_{pp}^{k\tau s} D_p(N_j I)] \triangleright_\Omega \\ K_{u\sigma}^{k\tau s i j} &= \triangleleft [D_p^T(N_i I) Z_{pn}^{k\tau s} N_j] \triangleright_\Omega + \\ & + \triangleleft [D_{n\Omega}^T(N_i I) E_{\tau s} N_j + E_{\tau,z} N_i N_j I] \triangleright_\Omega \\ K_{\sigma u}^{k\tau s i j} &= \triangleleft [N_i E_{\tau s} D_{n\Omega}(N_j I)] \triangleright_\Omega + \\ & + \triangleleft [E_{\tau s,z} N_i N_j I - N_i Z_{np}^{k\tau s} D_p(N_j I)] \triangleright_\Omega \\ K_{\sigma\sigma}^{k\tau s i j} &= \triangleleft [-N_i Z_{nn}^{k\tau s} N_j] \triangleright_\Omega. \end{aligned} \quad (28)$$

The complete fundamental nucleus for RMVT is the following 6×6 nucleus:

$$K^{k\tau sij} = \begin{bmatrix} K_{uu}^{k\tau sij} & K_{u\sigma}^{k\tau sij} \\ K_{\sigma u}^{k\tau sij} & K_{\sigma\sigma}^{k\tau sij} \end{bmatrix}. \quad (29)$$

5.3. Static problem

If the static problem is considered, the internal work must be equal to the external work. The external work of applied loadings can be written in terms of nodal quantities, according to the expansion in Eqn. (5) and to the discretization in Eqn. (19). The external load becomes:

$$\delta L_e^k = \delta q_{\tau i}^{kT} P_{\tau i}^k. \quad (30)$$

By imposing the definition of virtual variations, the following equilibrium conditions for the mixed case are obtained:

$$\begin{aligned} K_{uu}^{k\tau sij} q_{sj}^k + K_{u\sigma}^{k\tau sij} g_{sj}^k &= P_{\tau i}^k \\ K_{\sigma u}^{k\tau sij} q_{sj}^k + K_{\sigma\sigma}^{k\tau sij} g_{sj}^k &= 0 \end{aligned}. \quad (31)$$

6. Failure criteria

Composite materials are characterized by a mechanics and a failure mechanics which are more complicate in comparisons with conventional materials. A correct design requires an accurate and effective prediction of failure parameters, such as failure loadings, failure locations and failure indices. Highly accurate mechanical models are therefore needed to effectively describe the mechanics of composites and predict their failure. The RMVT model presented in this work is able to calculate all stresses with very high accuracy, and then particularly suitable for failure forecast. In this work, the maximum stress failure criterion has been adopted and is introduced (see Sec. 6.1). Further investigations could be part of future works, including other failure criteria, i.e. the criterion for composite laminates of Puck.

6.1. Maximum stress failure criterion

The idea of Maximum Stress criterion is to compare the lamina stress status with the lamina normal and shear strength. Failure occurs when the ratio is greater or equal to 1:

$$\begin{aligned} \frac{|\sigma_{11}|}{X} &\geq 1; & \frac{|\sigma_{23}|}{R} &\geq 1; \\ \frac{|\sigma_{22}|}{Y} &\geq 1; & \frac{|\sigma_{13}|}{S} &\geq 1; \\ \frac{|\sigma_{33}|}{Z} &\geq 1; & \frac{|\sigma_{12}|}{T} &\geq 1. \end{aligned} \quad (32)$$

X , Y , and Z represent the lamina normal strengths while R , S , and T are the lamina shear strengths in the material reference system (subscripts 23, 13, 12). Normal strengths depend on the sign of the corresponding stress component. In the case of tensile stresses, the tensile strengths X_T , Y_T and Z_T must be used in Eqn. (32). For negative values of the normal stress

components the compressive strengths X_C , Y_C and Z_C have to be used. Due to the linearity of the problem, a relation of proportionality holds between the applied loading $p_{zz}^{(0)}$ and every stress component. This means that, for every form of Eqn. (32), a failure loading $p_{zz}^{(F)}$ can be calculated with the following formula:

$$\begin{aligned} p_{zz,11}^{(F)} &= p_{zz}^{(0)} \frac{X}{|\sigma_{11}|}; & p_{zz,23}^{(F)} &= p_{zz}^{(0)} \frac{R}{|\sigma_{23}|}; \\ p_{zz,22}^{(F)} &= p_{zz}^{(0)} \frac{Y}{|\sigma_{22}|}; & p_{zz,13}^{(F)} &= p_{zz}^{(0)} \frac{S}{|\sigma_{13}|}; \\ p_{zz,33}^{(F)} &= p_{zz}^{(0)} \frac{Z}{|\sigma_{33}|}; & p_{zz,12}^{(F)} &= p_{zz}^{(0)} \frac{T}{|\sigma_{12}|}. \end{aligned} \quad (33)$$

The minimum failure load is the minimum value of Eqn. (33). Failure indices can be computed along the thickness z considering the minimum failure load as reference.

7. Numerical results

The benchmark proposed by Meyer Pieining in work [17] is proposed in the following. Two more plate problems are considered in the subsequent numerical investigations which are devoted to the calculation of the stress field and the failure index. The exact 3D solution of reference is provided by Pagano in work [3]. All FEM results shown in this paper are obtained in the MUL2 software with a regular 15×15 mesh of Q4 FEs. If not differently specified, three letter acronyms are used to identify the type of FEs employed in the analysis. The first letter is "E" or "L" in the case of ESL or LW variable descriptions, respectively. The second letter is "D" or "M" if PVD or RMVT are considered. The latter number identifies the order of the through-the-thickness expansion. For example, LM2 means that LW Mixed (RMVT) FEs with second order expansion through the thickness are considered.

7.1. Meyer-Piening benchmark

As a first example, the sandwich composite plate originally proposed by Meyer-Piening [17] is considered in Fig. 1. A localized transverse pressure is applied at the center of the top surface of the plate. The plate is simply supported at the four edges. The plate geometry is as follows: width $a=100$ [mm], length $b=200$ [mm], total thickness $h = 12$ [mm]. The faces of the same material have different thicknesses: top face thickness $h_3 = 0.1$ [mm], bottom face thickness $h_1 = 0.5$ [mm]. The core thickness is $h_1 = 11.4$ [mm]. The load consists of a transverse 1 [MPa] pressure applied to a rectangular zone at the center of the plate, which has dimensions of 5×20 [mm] (see Fig. 1). Such a loading situation is very common in practice. It occurs each time a concentrated loading is applied to a sandwich structure. The two faces have the following material data: $E_1 = 70000$ [MPa], $E_2 = 71000$ [MPa], $E_3 = 71000$ [MPa], $G_{13} = 26000$ [MPa], $G_{23} = 26000$ [MPa], $G_{12} = 26000$ [MPa], $\nu_{13} = 0.3$, $\nu_{23} = 0.3$,

$\nu_{12} = 0.3$. The core consists of metallic foam. Its material properties are: $E_1 = 3$ [MPa], $E_2 = 3$ [MPa], $E_3 = 2.8$ [MPa], $G_{13} = 1$ [MPa], $G_{23} = 1$ [MPa], $G_{12} = 1$ [MPa], $\nu_{13} = 0.25$, $\nu_{23} = 0.25$, $\nu_{12} = .25$. The results are collected in Tab. 2. The values of stresses and displacements are compared. 3D elasticity solutions as well as FE results obtained with 3D brick elements in MSC.NASTRAN have been compared to FE models developed in MUL2 code. LM2 represents a mixed LW FE with parabolic distribution of displacements in each layer. EMZC3 indicates a mixed ESL modelling with Zig-Zag and interlaminar Continuity capabilities. ED1 stands for ESL displacement formulated model with linear expansion for the whole sandwich plate. It appears clear that localized loadings require very accurate models even when a thin sandwich structure is under consideration. Moreover, single layer models are ineffective, even when a higher order form (EMZC3) is implemented.

7.2. Problem I

A four-edge simply supported orthotropic square plate with three layers made of the T300/5208 graphite/epoxy material is analyzed. Symmetric [0/90/0] and [0/45/0] as well as anti-symmetric [0/90/0/90] configurations are considered. The stacking sequence starts from the plate top; ply angles are measured with respect to the x -axis. In order to deal with thin and moderately thick plates, three different thickness ratios are considered: $a/h = 100, 50, 10$. A bi-sinusoidal pressure loading with a half wave for each side is addressed to. The mechanical properties of the material are listed below:

$$E_L = 132.5 \text{ MPa}, E_T = 10.8 \text{ MPa}, G_{LT} = 5.7 \text{ MPa},$$

$$G_{TT} = 3.4 \text{ MPa}, \nu_{LT} = 0.24, \nu_{TT} = 0.49. a = 1.0 \text{ m}.$$

The material strengths are:

$$X_t = 1515 \text{ MPa}, X_c = 1697 \text{ MPa}, Y_t = 43.8 \text{ MPa},$$

$$Y_c = 43.8 \text{ MPa}, Z_t = 43.8 \text{ MPa}, Z_c = 43.8 \text{ MPa},$$

$$R = 86.9 \text{ MPa}, S = 67.6 \text{ MPa}, T = 86.9 \text{ MPa}.$$

7.3. Problem II

A four-edge simply supported orthotropic square plate consisting of two layers [90/0] and three layers [0/90/0] with bi-sinusoidal pressure loading is considered. The thickness ratio $a/h = 10$. The geometric and material properties are:

$$a = 1.0 \text{ m}, E_L = 132.5 \text{ MPa}, E_T = 10.8 \text{ MPa},$$

$$G_{LT} = 5.7 \text{ MPa}, G_{TT} = 3.4 \text{ MPa},$$

$$\nu_{LT} = 0.24, \nu_{TT} = 0.49.$$

7.4. Stress field evaluation: Comparison between PVD and RMVT results

The results of different stresses of problem II are first considered in Tab. 3. Emphasis is placed on the top and bottom of the plate as well as on the interfaces between the layers. It can be seen that the results of transverse stresses obtained with the mixed formulation are almost exactly the same as Pagano's 3D solution. 3D results can also be obtained with the FEM solution for in-plane stresses. Results with models based on PVD show discontinuities for transverse stresses at the layer interfaces. Figs. 2-5 confirm the advantage of the "a priori" calculation of transverse stresses with RMVT. It can also be seen, in Fig. 4, that the transverse shear stresses σ_{13} appear in problem I with the classical PVD model, where it should be zero due to reasons of symmetry. This can have a significant effect on the calculation of failure, see the following section.

7.5. Results on maximum stress failure criteria

The results presented in this paper show the necessity of using mixed formulations for failure analysis. With PVD models, the wrong transverse shear stresses σ_{13} and σ_{23} appear in the center of the plate, which should be zero for problem II. These wrong stresses can be so high for thin plates that they reach the minimum failure load and lead to wrong results. The minimum failure load is not affected for thicker plates, but the numbers in the distribution of the failure index along the z -direction become not longer reasonable in some areas where these wrong transverse stresses are too high. Therefore, only mixed models should be used for running failure analysis. The results of the minimum first-ply failure loading values are presented in Tab. 4. LM models achieve very accurate results even with second order expansions. For most of the addressed cases, minimum failure load occurs in the central point of the plate. These locations along the z -direction can be dissimilar for different stacking-sequences. For the [0/45/0] case, the critical points are found in the layer interfaces which can be seen in Fig. 6, while for [0/90/0] and [0/90/0/90] failure occurs at the top of the plate (see Figs. 7,8). The results of [0/90/0] and [0/90/0/90] are compared with Pagano's 3D exact solution of reference [3]. Convergence for the minimum first-ply failure load is shown in Tab. 5. Furthermore, many analysis have been performed for the 3-layer case, with a step wise change of 15 deg. in the orientation of the middle layer. The results are shown in Fig. 9. It can be seen that the most critical point for failure in the z -direction depends to a great extent on the ply angles of the laminate and can change from the top to the interfaces of the lamination.

7.6. A global/scalar parameter for stress accuracy evaluation

In order to describe the performance of modelling stresses with a FEM model, it is necessary to consider all six stresses σ_{11} , σ_{22} , σ_{12} , σ_{13} , σ_{23} , σ_{33} and their distribution along z . If just particular stresses or particular locations in the thickness-direction are considered, the quality of a model cannot be described satisfactorily. Therefore, a simple global parameter for the accuracy of stresses of different FEM models has been adopted. The idea is to consider all six stresses and give their accuracy in comparison with a reference solution: the squared difference between the FEM and the reference solution is integrated numerically along z and the results is divided by the integral along z of the squared reference solution. This for each one of the six stress components. The result is multiplied by a factor of 100 in order to obtain the normalized percent error **ER** as a final value. The errors of all the stresses can then be summed to have a global indicator of solution fairness. According to this criterion, the results close to zero confirm a very accurate modelling (low error), while high values indicate that the model is not appropriate for the stress/failure index calculation. Tabs. 6,7 show the results of **ER** for problem II. The results are very accurate for plane stresses as nearly all the models provide an error of about 1% or even less. Considering transverse stresses, the error rises for all the PVD models, especially for ED1, whose solution is totally out of range. RMVT-based models are able to provide a very accurate description of transverse stresses. In particular, higher orders provide almost the exact solution for all six stresses. The ED1 results are the worst and the other theories all lie in-between. The dependency of **ER** on the lamination angle for different theories is also shown in Fig. 10. Different behaviors can be obtained with other theories.

8. CONCLUSIONS

The paper has shown the good performance of RMVT models for stress analysis. Several comparisons with classical PVD analysis are illustrated. All the analyses have been performed using MUL2 software, which is particularly useful to assess advanced FEs via comparisons with classical approaches. A new parameter for stress accuracy has been introduced. Particular emphasis has been given to the need for a mixed formulation in order to use failure criteria. The necessity of using mixed LW theories to obtain accurate stress results has been confirmed. Future works will address the application of the stress fields herein evaluated to progressive damage failure mechanisms.

REFERENCES

1. S.G. Lekhnitskii, "Anisotropic Plates", 2nd Edition, translated from the 2nd Russian Edition by Tsai S.W. and Cheron T., 1968.
2. N.J. Pagano, "Exact solutions for composite laminates in cylindrical bending", *Journal of Composite Materials*, Vol. 3, pp. 398-411, 1969.
3. N.J. Pagano, "Stress fields in composite laminates", *International Journal of Solids Structures*, Vol. 14, pp. 401-406, 1978.
4. R.K. Kapania and S. Raciti, "Recent advances in analysis of laminated beams and plates", *AIAA Journal*, Vol. 27, No. 7, pp. 923-946, 1989.
5. R.K. Kapania, "A review on the analysis of laminated shells", *Journal of Pressure Vessel Technology*, Vol. 11, No. 2, pp. 88-96, 1989.
6. A.K. Noor and W.S. Burton, "Assessment of shear deformation theories for multilayered composite plates", *Applied Mechanics Review*, Vol. 42, No. 1, pp. 1-18, 1989.
7. A.K. Noor and W.S. Burton, "Assessment of computational models for multilayered composite shells", *Applied Mechanics Review*, Vol. 43, No. 4, pp. 67-97, 1990.
8. J.N. Reddy, "Mechanics of laminated composite plates and shells, theory and analysis", *Applied Mechanics Review*, CRC Press, 2004.
9. P. Gaudenzi, R. Barboni and A. Mannini, "A finite element evaluation of single-layer and multi-layer theories for the analysis of laminated plates", *Composite structures*, Vol. 30, No. 4, pp. 427-440, 1995.
10. E. Reissner, "On a certain mixed variational theory and a proposed application", *International Journal for Numerical Methods in Engineering*, Vol. 20, pp. 1366-1368, 1984.
11. E. Carrera, "Developments, Ideas and Evaluations based upon the Reissner's Mixed Theorem in the modelling of multilayered plates and shells", *Applied Mechanics Review*, Vol. 54, pp. 301-329, 2001.
12. E. Carrera, "Theories and Finite Elements for Multilayered Anisotropic, Composite Plates and Shells", *Archives of Computational Methods in Engineering*, Vol. 9, pp. 87-140, 2002.
13. E. Carrera, "Evaluation of Layer-Wise Mixed Theories for Laminated Plates Analysis", *AIAA Journal*, No. 26, pp. 830-839, 1998.
14. E. Carrera, "Theories and Finite Elements for Multilayered Plates and Shells: A Unified Compact Formulation with Numerical Assessment and Benchmarking", *Archives of Computational Methods in Engineering*, Vol. 10, pp. 215-297, 2003.
15. E. Carrera, "Historical review of Zig-Zag theories for multilayered plates and shells", *Applied Mechanics Reviews*, Vol. 56, pp. 287-308, 2003.
16. L. De Masi and E. Carrera, "Classical and advanced multilayered plate elements based upon PVD and RMVT. Part 1. Derivation of finite element matrices", *International Journal Numerical Methods in Engineering*, Vol. 55, pp. 191-231, 2002.
17. H.M. Meyer Piening, "Experience with "Exact" linear sandwich beam and plate analysis regarding bending instability and frequency investigation", *Proc. of the fifth International Conference on Sandwich Constructions*, Switzerland, September 5-7, 37-48, 2000.

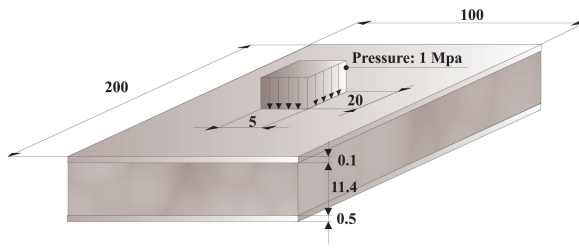


Figure 1. Meyer–Piening rectangular sandwich plates subjected to transverse pressure located at the plate center.

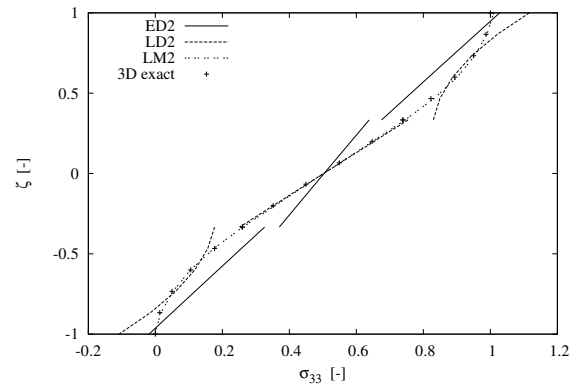


Figure 4. σ_{33} in the center of the plate along thickness ζ ; $a/h = 10$, $[0/90/0]$; Problem I

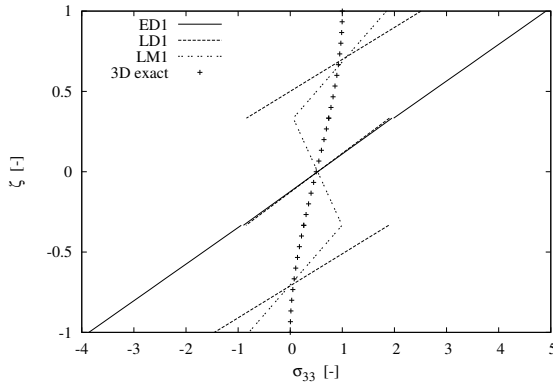


Figure 2. σ_{33} in the center of the plate along thickness ζ ; $a/h = 10$, $[0/90/0]$; Problem I

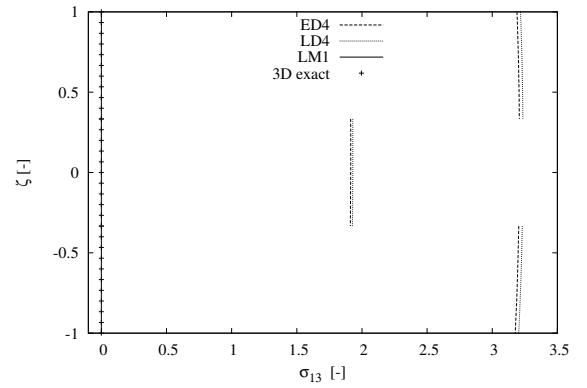


Figure 5. σ_{13} in the center of the plate along thickness ζ ; $a/h = 10$, $[0/90/0]$; Problem I

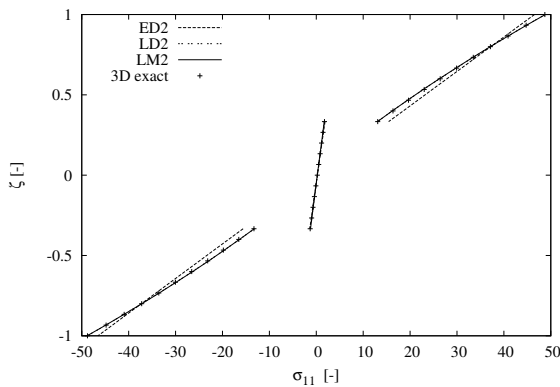


Figure 3. σ_{11} in the center of the plate along thickness ζ ; $a/h = 10$, $[0/90/0]$; Problem I

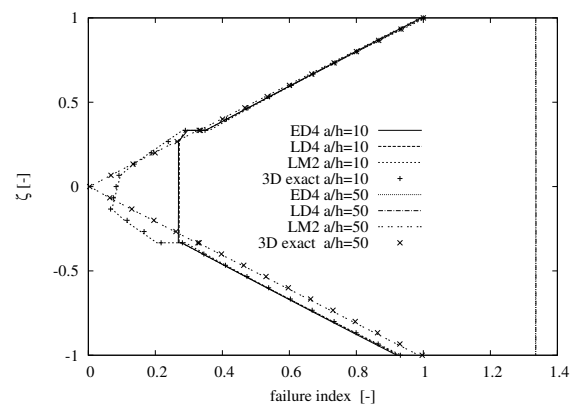


Figure 6. Failure index via max stress criterion along thickness ζ ; $[0/90/0]$, $a/h = 10$, $a/h = 50$; Problem I

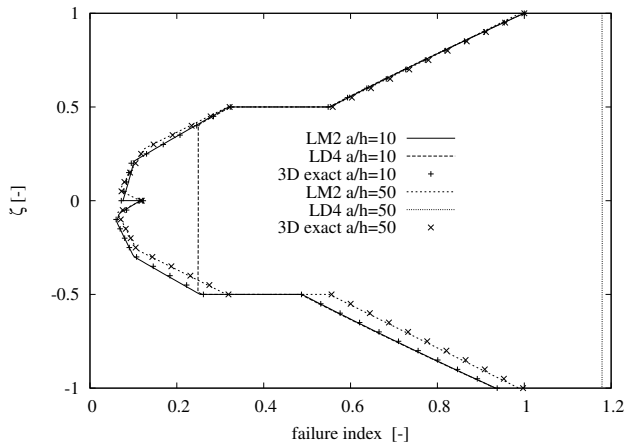


Figure 7. Failure index via max stress criterion along thickness ζ ; $[0/90/0/90]$, $a/h = 10$ and $a/h = 50$; Problem I

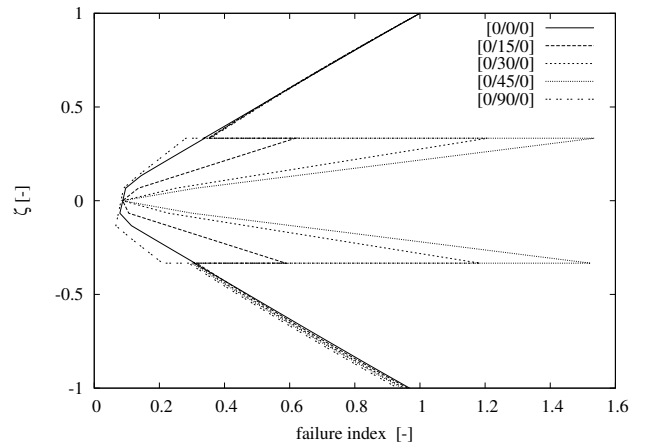


Figure 9. Failure index via max stress criterion along ζ for various lamination angles; $a/h = 10$, minimum failure load at the top; LM2 model; Problem II

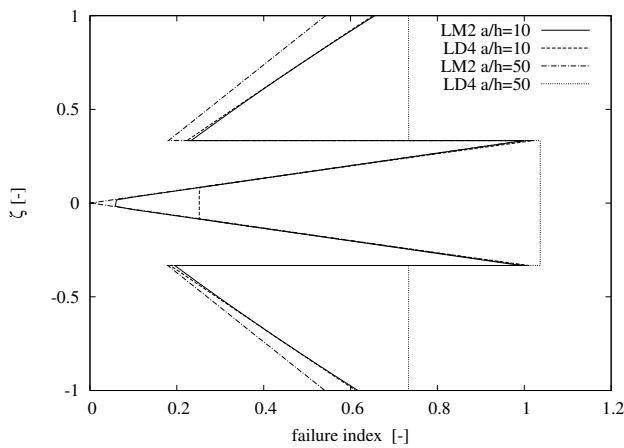


Figure 8. Failure index via max stress criterion along thickness ζ ; $[0/45/0]$, $a/h = 10$, $a/h = 50$; Problem I

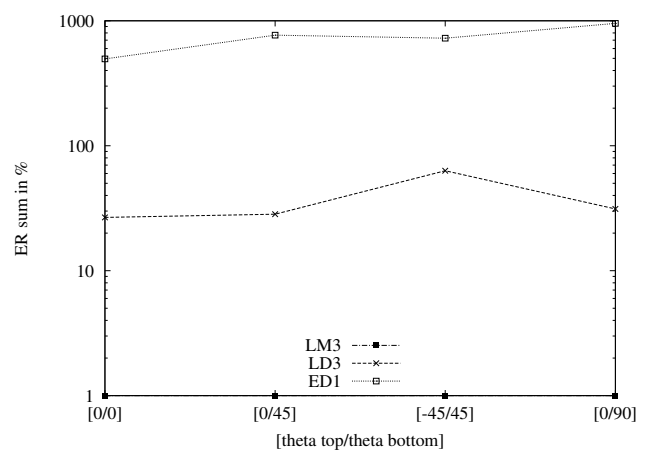


Figure 10. Dependency of ER on the lamination angle theta, LM3 results as reference; Problem II

1st order
$F_t = (1 + \zeta)/2$
$F_b = (1 - \zeta)/2$
2nd order
$F_t = -(1 + \zeta)(\zeta - z_1)/(2(-1 + z_1))$
$F_2 = (-1 + \zeta^2)/(-1 + z_1^2)$
$F_b = (-1 + \zeta)(\zeta - z_1)/(2(1 + z_1))$
3rd order
$F_t = (1 + \zeta)(\zeta - z_1)(\zeta - z_2)/(2(-1 + z_1)(-1 + z_2))$
$F_2 = -(-1 + \zeta)(1 + \zeta)(\zeta - z_1)/((z_1 - z_2)(-1 + z_2^2))$
$F_3 = (-1 + \zeta)(1 + \zeta)(\zeta - z_2)/((-1 + z_1^2)(z_1 - z_2))$
$F_b = -(-1 + \zeta)(\zeta - z_1)(\zeta - z_2)/(2(1 + z_1)(1 + z_2))$
4th order
$F_t = -(1 + \zeta)(\zeta - z_1)(\zeta - z_2)(\zeta - z_3)/(2(-1 + z_1)(-1 + z_2)(-1 + z_3))$
$F_2 = (-1 + \zeta)(1 + \zeta)(\zeta - z_1)(\zeta - z_2)/((z_1 - z_3)(z_2 - z_3)(-1 + z_3^2))$
$F_3 = -(-1 + \zeta)(1 + \zeta)(\zeta - z_1)(\zeta - z_3)/((z_1 - z_2)(-1 + z_2^2)(z_2 - z_3))$
$F_4 = (-1 + \zeta)(1 + \zeta)(\zeta - z_2)(\zeta - z_3)/((-1 + z_1^2)(z_1 - z_2)(z_1 - z_3))$
$F_b = (-1 + \zeta)(\zeta - z_1)(\zeta - z_2)(\zeta - z_3)/(2(1 + z_1)(1 + z_2)(1 + z_3))$

Table 1
Base functions $F_r(\zeta)$ with Lagrange Polynomials up to 4th order

	z	u_3 [mm]	σ_{22} [MPa]	σ_{11} [MPa]	σ_{12} [MPa]
Upper Face					
3D Analytical	top	-3.78	-241	-624	0
	bottom		211	580	0
3D-NASTRAN	top	-3.84	-237	-628	0
	bottom		102	582	0
2D-LM2	top	-3.7628	-223.93	-595.56	0
	bottom		196.37	556.00	0
2D-EMZC3 present	top	-2.0483	-122.59	-214.27	0
	bottom		99.62	181.40	0
2D-ED1	top	-0.0187	-23.99	-29.46	0
	bottom		-23.75	-29.17	0
Lower Face					
3D Analytical	top		-121	-138	0
	bottom	-2.14	127	146	0
3D-NASTRAN	top		-120	-140	0
	bottom	-2.19	127	148	0
2D-LM2	top		-118.99	-136.20	0
	bottom	-2.1403	125.00	144.03	0
2D-EMZC3 present (RMVT-1)	top		-190.7	-227.67	0
	bottom	-1.8717	191.11	230.76	0
2D-ED1	top		3.32	4.87	0
	bottom	-0.0181	4.50	6.36	0

Table 2
Comparison of different analysis: Meyer-Piening benchmark

ζ	σ_{33}		σ_{33}		σ_{11}		σ_{11}	
	ED2	LD2	LM2	3D Pagano	ED2	LD2	LM2	3D Pagano
1.000000	1.028	1.116	1.009	1.000	46.53	48.78	48.73	48.74
0.866667	0.957	1.021	0.990	0.987	40.30	40.93	40.92	40.88
0.733333	0.886	0.945	0.954	0.950	34.08	33.43	33.38	33.47
0.600000	0.816	0.887	0.901	0.894	27.86	26.28	26.23	26.42
0.466667	0.745	0.849	0.831	0.822	21.64	19.48	19.45	19.66
0.333333	0.675	0.830	0.746	0.739	15.43	13.03	13.05	13.10
0.333333	0.638	0.754	0.746	0.739	1.86	1.69	1.74	1.74
0.200000	0.584	0.653	0.648	0.647	1.21	1.11	1.13	1.13
0.066667	0.530	0.552	0.551	0.549	0.56	0.52	0.53	0.52
-0.066667	0.477	0.452	0.454	0.449	-0.09	-0.06	-0.07	-0.09
-0.200000	0.423	0.352	0.357	0.351	-0.75	-0.65	-0.67	-0.70
-0.333333	0.370	0.252	0.261	0.260	-1.40	-1.23	-1.27	-1.31
-0.333333	0.326	0.177	0.261	0.260	-15.60	-13.20	-13.22	-13.28
-0.466667	0.257	0.156	0.175	0.177	-21.80	-19.63	-19.60	-19.82
-0.600000	0.188	0.118	0.105	0.106	-27.99	-26.40	-26.35	-26.56
-0.733333	0.119	0.061	0.052	0.050	-34.18	-33.53	-33.48	-33.58
-0.866667	0.050	-0.015	0.016	0.013	-40.37	-41.00	-40.99	-40.97
-1.000000	-0.019	-0.108	-0.002	0.000	-46.56	-48.81	-48.77	-48.79

Table 3
 σ_{33} and σ_{11} at the center of the plate along thickness ζ ; $a/h = 10$, $[0/90/0]$; Problem I

a/h [MPa]	100 $\times 10^{-2}$	50 $\times 10^{-1}$	10 $\times 1$
Analytical			
3D Pagano	9.1838	3.6434	7.2858
MUL2, Q4, 8×8			
<i>Classical ESL models</i>			
ED1	3.6496*	2.6682*	5.9578
ED2	3.4410*	2.7355*	7.7215
ED3	3.4386*	2.7280*	7.1818
ED4	3.4386*	2.7280*	7.3307
<i>Classical LW models</i>			
LD1	3.4620*	2.7470*	6.5592
LD2	3.4382*	2.7268*	7.2457
LD3	3.4382*	2.7267*	7.2847
LD4	3.4382*	2.7267*	7.2901
<i>Mixed LW models</i>			
LM1	8.2752	3.2824	6.5338
LM2	9.2822	3.6798	7.2344
LM3	9.2829	3.6805	7.2579
LM4	9.2829	3.6807	7.2613

(*)Minimum failure loading due to wrong transverse shear stresses

Table 4
 Minimum first-ply failure loading values; $[0/90/0]$ stacking sequence; Problem I

[MPa]	$a/h = 100$ $\times 10^{-2}$	$a/h = 50$ $\times 10^{-1}$	$a/h = 10$ $\times 1$
3D Pagano	9.1838	3.6434	7.2858
Q4, 6×6	9.3656	3.7106	7.2115
Q4, 8×8	9.2822	3.6798	7.2344
Q4, 10×10	9.2455	3.6660	7.2432

Table 5

Convergence of first-ply failure loading values with Maximum Stress Criterion; [0/90/0] stacking sequence, LM2 results; Problem I.

	$ER(\sigma_{11})$ ($a/2, a/2$)	$ER(\sigma_{22})$ ($a/2, a/2$)	$ER(\sigma_{12})$ (0, 0)	$ER(\sigma_{13})$ (0, $a/2$)	$ER(\sigma_{23})$ ($a/2, 0$)	$ER(\sigma_{33})$ ($a/2, a/2$)	sum
Classical ESL							
ED1	1.85	1.95	1.65	37.74	37.38	873.07	953.6
ED2	1.33	1.31	0.61	34.22	34.19	46.07	117.7
ED3	0.72	0.73	0.35	18.78	19.20	38.69	78.5
ED4	0.62	0.63	0.22	17.75	18.07	33.43	70.7
Classical LW							
LD1	3.73	3.79	2.38	34.56	34.54	371.59	450.6
LD2	0.79	0.80	0.43	22.74	23.17	8.19	56.1
LD3	0.13	0.13	0.02	13.08	13.33	4.55	31.2
LD4	0.12	0.12	0.02	13.08	13.33	3.63	30.3
Mixed LW							
LM1	5.82	5.94	1.11	30.71	30.44	8.59	82.6
LM2	0.88	0.89	0.49	14.15	14.41	2.51	33.3
LM3	0.46	0.46	0.39	0.92	0.92	0.36	3.5

Table 6

ER in % for all the six stresses; stacking sequence [90/0] (top-to-bottom); Pagano 3D solution as reference; Problem II

	$ER(\sigma_{11})$ ($a/2, a/2$)	$ER(\sigma_{22})$ ($a/2, a/2$)	$ER(\sigma_{12})$ (0, 0)	$ER(\sigma_{13})$ (0, $a/2$)	$ER(\sigma_{23})$ ($a/2, 0$)	$ER(\sigma_{33})$ ($a/2, a/2$)	sum
Classical ESL							
ED1	4.76	4.98	2.77	49.51	40.35	403.17	505.5
ED2	4.46	4.25	2.89	48.41	36.34	13.01	109.4
ED3	0.83	0.93	0.71	20.55	21.70	17.18	61.9
ED4	0.91	0.43	0.71	20.57	21.75	4.63	49.0
Classical LW							
LD1	1.37	4.80	0.95	23.47	30.13	140.56	201.3
LD2	0.19	0.55	0.15	5.68	21.16	4.03	31.8
LD3	0.05	0.24	0.09	4.79	19.52	2.02	26.7
LD4	0.05	0.24	0.09	4.79	19.52	1.97	26.7
Mixed LW							
LM1	2.46	5.93	1.38	4.92	22.06	71.29	108.0
LM2	0.41	0.63	0.44	3.01	7.53	0.52	12.5
LM3	0.21	0.33	0.35	0.42	0.63	0.31	2.3

Table 7

ER in % for all the six stresses; stacking sequence [0/90/0]; Pagano 3D solution as reference; Problem II